Solid State Phenomena
ISSN: 1662-9779, Vol. 353, pp 109-114
doi:10.4028/p-n7CbIP

Submitted: 2023-06-01
Accepted: 2023-08-21
Online: 2023-12-05

Crystal-Defect-Associated Transformation Strain Paths of Electric Current Pulse (ECP) Induced α to β Transformation in Cu-40%Zn

Meishuai Liu[1,2,a], Claude Esling[1,b*], Yudong Zhang[1,c], Benoit Beausir[1,d], Xinli Wang[2,e], Xiang Zhao[2,f] and Liang Zuo[2,g]

[1]Laboratoire d'Étude des Microstructures et de Mécanique des Matériaux (LEM3), CNRS UMR 7239, Université de Lorraine, Metz 57070, France

[2]Key Laboratory for Anisotropy and Texture of Materials (Ministry of Education), Northeastern University, Shenyang 110819, China

[a]13694120612@163.com, [b]claude.esling@univ-lorraine.fr, [c]yudong.zhang@univ-lorraine.fr, [d]benoit.beausir@univ-lorraine.fr, [e]wangxl@research.neu.edu.cn, [f]zhaox@mail.neu.edu.cn, [g]lzuo@mail.neu.edu.cn.

Keywords: Electric current pulse (ECP), Phase transformation, Orientation relationship, Crystal defect.

Abstract. A systematic study has been made on a Cu-40%Zn alloy treated by an electric current pulse (ECP) and by the examination of the microstructure and the crystallographic features of both the parent and the product phases. The β precipitates under ECP show a Kurdjumov Sachs Orientation Relation (K-S OR) in the vicinity of the grain boundaries (GBs), but a Nishiyama Wasserman (N-W) OR within the grains. Along the GBs the $\{111\}_\alpha$ /$<1\bar{1}0>_\alpha$ dislocation arrays were spotted, whereas the $\{111\}_\alpha$ /$<11\bar{2}>_\alpha$ stacking faults were observed in the grain interiors. A closer examination of the lattice strain required for the phase transformation revealed that the maximum lattice deformation under the K-S OR is a shear on the $\{111\}_\alpha$ plane in the $<1\bar{1}0>_\alpha$ direction. The dislocations arrays existing along the GBs offer the pre-strain that favors the precipitation of β particles obeying the K-S OR. Oppositely, the stacking faults within the grains provide pre-stains for the formation of the β precipitates respecting the N-W OR. This study sheds some light on the mechanisms by which crystal defects initiate phase transformation in a Cu-40%Zn alloy.

Introduction

The ECP treatment as an effective, high-speed, and short duration approach can realize ultra-rapid heating (heating rate about 10^6–10^7 K/s) [1] and cooling [1-4] of a bulk material, allowing to retain the high-temperature phase to the room temperature [5-11] and offering possibility for the study of phase transformation. Prior studies have already proven the capacity of ECP treatment for phase transformation [1-15].

In the past, we found that the ECP was capable of inducing phase transformation in the Cu-Zn systems and the induced β precipitates could be retained to the room temperature [12-15]. As we know, specific orientation relationships (ORs) will be respected by the two end phases and the different type of the defects contribute to minimize the lattice distortion energy during the phase transformation process [16-20]. Thus, in this paper, a thorough study of the microstructure, phase transformation ORs and the transformation strain of the α to β heating phase transformation was conducted in an annealed Cu-40%Zn alloy treated ECP treatments.

Experiments

The material used in the present work is as-hot-rolled Cu-40%Zn. Dog-bone-shaped samples with gauge dimensions of 10mm in length, 2mm in width, and 1.5mm in thickness were machined and heat treated at 500°C (in the α+β phase region) for 30 min then cooled in air to increase the crystal perfection. After annealing, the samples were further treated by ECPs. The ECP treatment setup is illustrated in Fig.1. A discharge of the capacitor banks after charging produced a single electric

current pulse and was applied directly to the sample. The treatment was performed at room temperature and under atmospheric condition. In this work, the ECP treatment was performed at two instant voltages that correspond to the current densities of about 16.21 kA/ mm^2 and 17.13 kA/ mm^2.

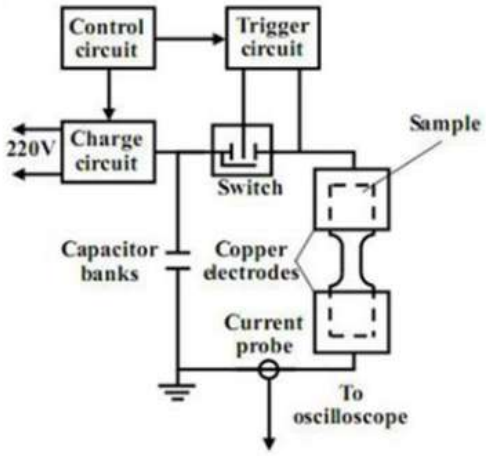

Fig. 1. The ECP experimental set up

The microstructural examinations and crystallographic orientation investigations were performed using a Jeol JSM 6500 F SEM equipped with an EBSD acquisition camera and the Aztec online acquisition software package (Oxford Instruments). The EBSD measurements were conducted at a step size of 0.15 μm and under an accelerating voltage of 15 kV. The EBSD data were analyzed with the Oxford Channel 5 software and the Atex software [21]. The EBSD samples were electrolytically polished in a solution of 20 % (volume fraction) nitric acid in methanol at 18 V for 3 seconds at room temperature. The dislocations and stacking faults were analyzed using a Philips CM 200 transmission electron microscope (TEM) operated at 200 kV. TEM thin foils were prepared first by mechanical thinning to 80 μm and then by electrolytic polishing to perforation at -30°C in the same solution at 20 V, using a Struers Tenupol-5 twin-jet electropolisher.

Results and Discussion

Fig. 2 shows the EBSD maps of the annealed and the ECPed (j_{max}= 16.21 kA/ mm^2 and j_{max}= 17.13 kA/ mm^2) Cu-40%Zn samples. In the figures, the α grains are in gray (EBSD band contrast) and the β particles are in color (according to their crystallographic orientations). In the annealed state, the microstructure is mainly composed of α phase with some β grains located at the α grain boundaries and triple-junctions, as shown in Fig. 2 (a). After the ECP treatments, some fine β precipitates appear along the α phase grain boundaries and in grain interiors, as shown in Fig. 2 (b) and (c). With the increase of the electric current density, the amount and the size of the β precipitates increase.

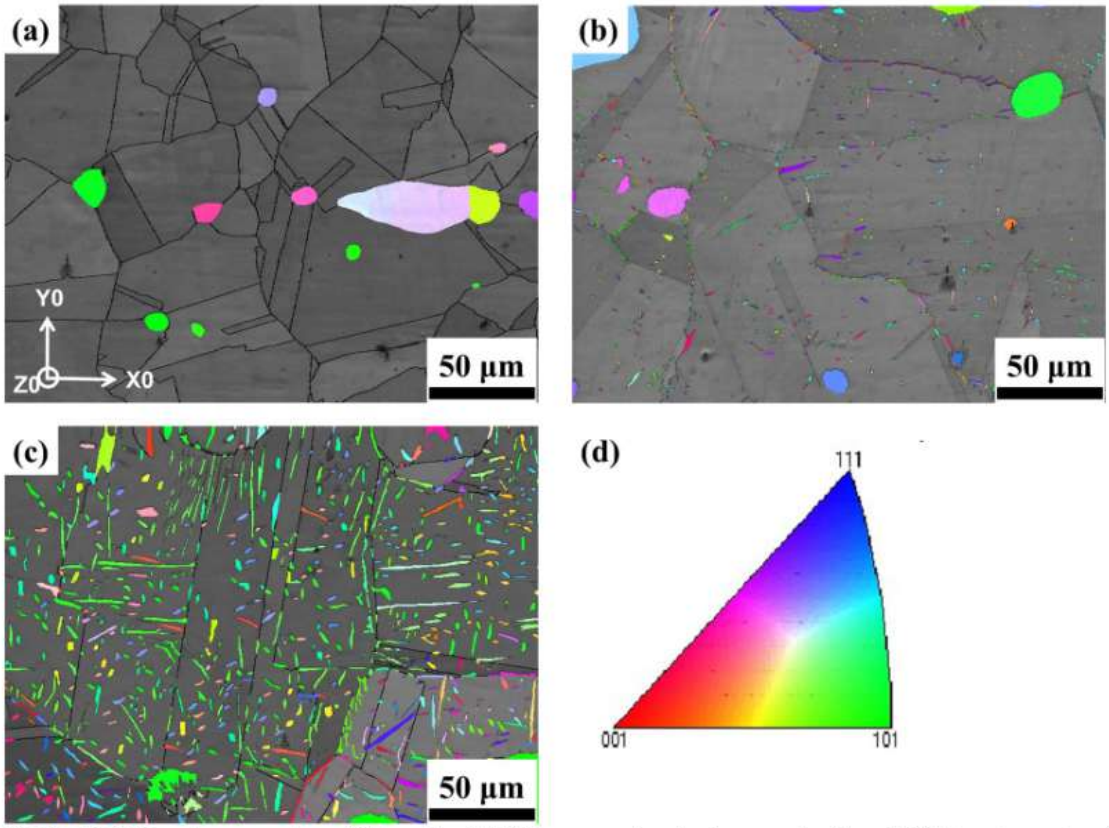

Fig. 2. SEM-EBSD micrographs of the Cu-40%Zn samples before and after ECP treatments. (a) The annealed sample. (b) The ECPed sample treated with current density j_{max}= 16.21 kA/ mm² and (c) j_{max}= 17.13 kA/ mm². (d) The X0 IPF color code. The electric current direction is in X0.

Table 1. The amount of β_{GI} and β_{GB} that obey different transformation ORs (the K-S and the N-W) and at different angular deviations from the exact OR, obtained under different ECP treatments.

	Electric current density (kA/mm^2)	OR	0-5°	>5°
α / β_{GB}	16.21	K-S	79.3%	1.2%
		N-W	19.5%	
	17.13	K-S	76.3%	1.1%
		N-W	22.6%	
α / β_{GI}	16.21	K-S	20.6%	1.2%
		N-W	78.2%	
	17.13	K-S	16.9%	1.8%
		N-W	81.3%	

To evaluate the orientation relationship characteristics, a large number of α and β precipitates were selected for the crystallographic analysis, using the measured orientations of the parent α phase and the β precipitates. It was found that one part of β precipitates respects the N-W OR ($\{111\}_\alpha // \{110\}_\beta$, $<11\bar{2}>_\alpha // <\bar{1}10>_\beta$) with the surrounding α phase, whereas the other part respects the K-S OR ($\{111\}_\alpha // \{110\}_\beta$, $<\bar{1}10>_\alpha // <\bar{1}11>_\beta$) with the neighboring α phase. Table 1 shows the detailed results of the OR and the corresponding angular deviations from the exact OR. Hereafter, we denote the ECP induced β precipitates located along the α grain boundaries β_{GB}, whereas those located in the α grain interiors β_{GI}. It can be found that most β_{GB} (up to 79.3%) respects the K-S OR, whereas most β_{GI} (up to 81.3%) obeys the N-W OR with the parent α phase. That means the β precipitates obeys the K-S OR when formed along the α grain boundaries, or the N-W OR when formed in the α grain interiors.

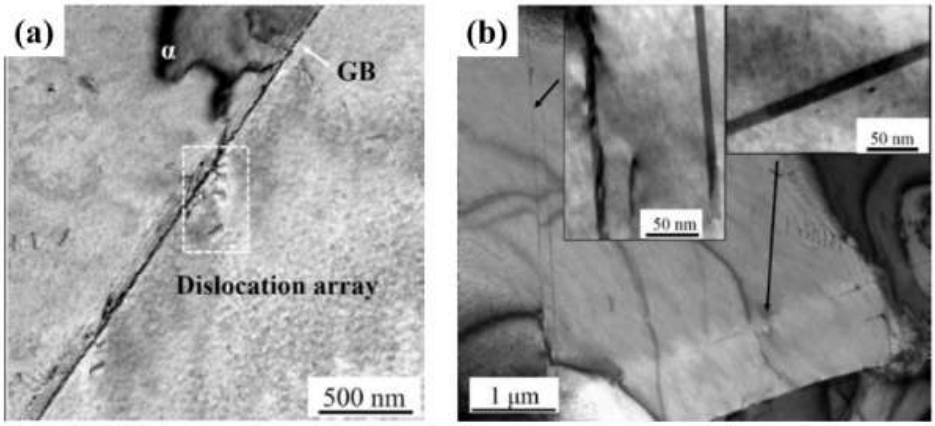

Fig. 3. TEM bright field images of crystal defects along α grain boundaries and in α grain interiors. (a) dislocation arrays, (b) stacking faults.

To find out the origins of such precipitation-location-related OR change, we investigated the sub-structure details of the α phase in the two locations in the annealed Cu-40%Zn alloy by TEM. The examination results revealed that parallel dislocation arrays with $\{111\}_\alpha<1\bar{1}0>_\alpha$ type are mainly located along the α grain boundaries and the $\{111\}_\alpha<11\bar{2}>_\alpha$ type stacking faults are observed within the α interiors, as shown with a typical example in Fig. 3 (a) and (b). This indicates that the OR change may be related to the different kinds of crystal defects existing before the ECP treatment, as different kinds of crystal defects represent different kinds of lattice deformation in the α phase. Thus, we further analyzed the lattice deformation associated with the α to β transformation.

Table 2. Deformation gradient tensor of the structure deformation to form the β precipitates in the sample treated under j = 17.28 kA/ mm^2 under the K-S and under the N-W OR expressed in the K-S and the N-W OR reference frame, respectively.

OR	Deformation Gradient Tensor		
	$i//[\bar{1}\bar{1}2]_\alpha$	$j//[1\bar{1}0]_\alpha$	$k//[111]_\alpha$
K-S	$\begin{bmatrix} 1.0614 & 0 & 0.1760 \\ -0.1760 & 0.9667 & 0.2638 \\ 0 & 0 & 0.9667 \end{bmatrix}$		
	$i//[1\bar{1}0]_\alpha$	$j//[11\bar{2}]_\alpha$	$k//[111]_\alpha$
N-W	$\begin{bmatrix} 1.1109 & 0 & 0 \\ 0 & 0.9137 & 0.3230 \\ 0 & 0 & 0.9691 \end{bmatrix}$		

In the present work, the transformation happened from the α phase with an FCC structure to the β precipitates having a BCC structure under two different ORs (K-S and N-W). By examining the lattice correspondences between the two phases under the two different ORs, we resolved the lattice strains under the two different ORs and expressed them in the deformation gradient tensor in the corresponding OR reference systems, as displayed in Table 2. It is seen that for the formation of the K-S β phase, it requires the largest shear strains on the $\{111_\alpha$ plane in the $<1\bar{1}0>_\alpha$ direction, which corresponds to the $\{111\}_\alpha/<1\bar{1}0>_\alpha$ slip system. For the N-W β precipitates, the required maximum deformation is a shear on the $\{111_\alpha$ plane in the $<11\bar{2}>_\alpha$ direction, a shear that corresponds to the $\{111\}_\alpha/<11\bar{2}>_\alpha$ partial slip system. Thus, the existing $\{111\}_\alpha/<1\bar{1}0>_\alpha$ dislocation arrays provide the favorable pre-strains that can decrease the lattice deformation of the transformation, hence facilitate the formation of the β precipitates obeying the K-S OR, whereas the $\{111\}_\alpha/<11\bar{2}>_\alpha$ stacking faults offer the favorable pre-strains that can reduce the transformation deformation, thus enhance the formation of the β precipitates respecting the N-W OR. As a result, the different kinds of crystal defects in the α phase existing before the ECP treatments gave rise to the selection of the different ORs for the α to β transformation.

[15] M.S. Liu, Y.D. Zhang, X.L. Wang, B. Beausir, X. Zhao, L. Zuo, C. Esling, Crystal defect associated selection of phase transformation orientation relationships (ORs). Acta Mater. (2018) 315-326.

[16] Y. L. He, S. Godet, P. J. Jacques, J. J. Jonas, Crystallographic relations between face-and body-centred cubic crystals formed under near-equilibrium conditions: observations from the Gibeon meteorite. Acta Mater. 54 (2006) 1323-1334.

[17] D. De Knijf, T. Nguyen-Minh, R. H. Petrov, L. A. I. Kestens, J. J. Jonas, Orientation dependence of the martensite transformation in a quenched and partitioned steel subjected to uniaxial tension. J. Appl. Crystallogr. 47 (2014) 1261-1266.

[18] J.J. Jonas, Y.L. He, S. Godet, The possible role of partial dislocations in facilitating transformations of the Nishiyama-Wassermann type. Scripta Mater. 52 (2005) 175-179.

[19] N. J. Wittridge, J. J. Jonas, J. H. Root, A dislocation-based model for variant selection during the γ-to-α' transformation. Metall. Mater. Trans. A 32 (2001) 889-901.

[20] H. J. Bunge, W. Weiss, H. Klein, L. Wcislak, U. Garbe, J. R. Schneider, Orientation relationship of Widmannstätten plates in an iron meteorite measured with high-energy synchrotron radiation. J. Appl. Crystallogr. 36 (2003) 137-140.

[21] B. Beausir, J.-J. Fundenberger, ATEX-Software, Analysis Tools for Electron and X-ray Diffraction. Université de Lorraine, Metz, 2017 on http://www.atex-software.eu